

Article

Analysis of Different Mould Section Sizes to Optimize the Submerged Entry Nozzle to Measure the Meniscus Fluctuation in a Continuous Casting Mould

Manish Kumar *, Praveen Mishra and Apurba Kumar Roy

Department of Mechanical Engineering, Birla Institute of Technology, Mesra, Ranchi 835215, India; pmishra@bitmesra.ac.in (P.M.); akroy@bitmesra.ac.in (A.K.R.)

* Correspondence: manishkr159@gmail.com

Abstract: An experimental investigation has been carried out to analyse different mould section sizes to measure the meniscus fluctuation by varying different liquid flow rates and different submerged entry nozzle port angles, i.e., 0° port angles, 15° downward and 15° upward port angles. The terms of maximum surface wave fluctuation and standard deviation have been analysed for the above mentioned parameters. It was observed that a submerged entry nozzle with 0° port was found to be superior when it was compared with a 15° downward and 15° upward port nozzle. By conducting an experiment, it was observed that as the water flow rate increased, the maximum wave amplitude was found to be increasing, which results in more turbulence. Different mould section sizes were analysed to provide background information to the steelmaker to analyse the behaviour of fluid flow pattern. The operating parameters of the result obtained from the present setup were compared with the published literature, and a scale down of slab moulds can be justified regarding the rough flow pattern in the mould but can lack accuracy. The reason behind this statement is that the integral length scales of the turbulent flow between scaled down and full scale models can be different. Therefore, details of the flow pattern can become great differences between both types of models.

Keywords: continuous casting process; submerged entry nozzle; mould; submergence depth; well depth; wave fluctuation



Citation: Kumar, M.; Mishra, P.; Roy, A.K. Analysis of Different Mould Section Sizes to Optimize the Submerged Entry Nozzle to Measure the Meniscus Fluctuation in a Continuous Casting Mould. *Crystals* **2021**, *11*, 564. <https://doi.org/10.3390/cryst11050564>

Academic Editor: Umberto Prisco

Received: 31 December 2020

Accepted: 30 March 2021

Published: 19 May 2021

Publisher's Note: MDPI stays neutral with regard to jurisdictional claims in published maps and institutional affiliations.



Copyright: © 2021 by the authors. Licensee MDPI, Basel, Switzerland. This article is an open access article distributed under the terms and conditions of the Creative Commons Attribution (CC BY) license (<https://creativecommons.org/licenses/by/4.0/>).

1. Introduction

Over five decades, a large number of investigations have been carried out on various aspects of the continuous casting process. It is known that there are four recirculating domains inside the mould, two above the nozzle port and two below the nozzle port. The lower two recirculating domains are much bigger in size than those of the upper two recirculating domains. The first study was conducted on the straight bore nozzle and it studied the behaviour of the fluid flow pattern in the submerged entry nozzle with the help of a stopper rod and the slide gate control system. For most of the possible cases, modelling is done using water as the fluid which represents molten steel, as shown in Table 1: water at 20 °C and liquid steel at 1600 °C have practically equal kinematic viscosities, thus making reduced scale aqueous models an excellent tool for the investigation of fluid flow process inside the mould for steelmaking to produce a better quality steel. Moreover, when water is used as a fluid representing molten steel, it fully ensures that easy flow visualization in the system.

The control of the level of fluctuations in the mould is mostly influenced by the Submerged Entry Nozzle (SEN) which plays a vital role in it. The parameters which mostly affect the submerged entry nozzle (SEN) are the internal bore diameter, port geometry, port locations, number of ports, internal base design, well depth, SEN submergence depth, SEN position, argon injection rate, tundish flow control, mould geometry, superheat, and casting speed. To decrease the level of fluctuation and avoid slag entrainment can be

achieved by suitable SEN design [1]. Fang et al. studied the effects of a Submerged Entry Nozzle on flow and beginning solidification in a continuous casting bloom form with electromagnetic stirring. The exploratory and mathematical results indicated that the optimized four-port SEN with inclining establishment cannot just improve the fluid flow pattern by lightening the level variance and diminishing the impact pressure to the wall [2]. Cui et al. studied the impact of the submerged entry nozzle structure on liquid flow in a beam blank continuous casting mould. The outcomes show that the stream under the single-port SEN prompts a too critical effect on the solidifying shell in the area of the rib centre and the filets, particularly the filet of the external bend [3].

Table 1. Physical property of water and steel at 20 °C and 1600 °C, respectively.

| Property | Water (20 °C) | Steel (1600 °C) |
|--|------------------|--------------------------|
| Molecular viscosity, kg/ms | 0.001 | 0.0064 |
| Density, kg/m ³ | 1000 | 7014 |
| Kinematic viscosity, m ² /s | 10 ⁻⁶ | 0.913 × 10 ⁻⁶ |
| Surface tension, N/m | 0.073 | 1.6 |

Ramirez and Trejo studied the fluctuations of the free surface of liquid steel; two different models with the same casting parameters with different thicknesses were analysed by the hydrodynamics behaviour at the top portion of the mould. The first model was the standard thickness slab and the second model had a thickness three times wider [4]. Michalek et al. designed submerged entry nozzles having one that was a straight conventional nozzle and a second one having five ports. According to the author, the riddling depth of the newest steel was observed with the help of straight SEN having a largest value of 5.6 m [5]. In Liu et al., a model was introduced for studying the transient flow during continuous casting and it was, according to the author, for simulation of multiple stopper rod movement. The model taken into consideration comprises four sub models for studying transient flow conditions [6]. Ramirez et al. suggested that SEN clogging was a complex problem in the continuous casting of steel which decreases the quality of steel produced. The clogging increases gradually which generates insufficient and uneven fluid flow patterns inside the nozzle and mould [7]. Cho et al. studied the fluid flow behaviour in the mould that was not stable which induces surface velocity and fluctuations levels and relevance slag, which lead to defects in the surface in the continuous casting of steel. In this work, nail board dipping quantities were active to enumerate transient surface level, the velocity at the surface, the direction of flow, and depth of slag [8].

Li et al. observed the latest method for the swirling flow in SEN. For inducing swirling flow, a rotating electromagnetic field was build up all around the SEN with the help of Lorentz force. The influence of the structure of the nozzle on the flow and temperature around the SEN and mould and even the influence of coil current intensity were numerically simulated [9]. Begum et al. investigated a 3D computational fluid dynamics (CFD) model with turbulent fluid flow condition developed for the simulation of an industrial-sized vertical direct chill slab caster [10]. Ren et al. suggested a method based on particle analysis for studying the non-metallic inclusions in steel produced. For a short period, when compared with traditional methods, the process had the advantages of morphology, size measuring, original positions recording, and, for a particular area, identifying the composition of non-metallic inclusions [11]. Yingnakorna and Khumkoaa suggested that preheating SEN itself was an important factor which determines the lifetime of SEN. In this research, they investigated the corrosion behaviour and lifetime of SEN [12]. Pirker et al. investigated flow behaviour in the submerged entry nozzle as crucial for continuous slab casting because it controls the mould fluid flow pattern. Here, the bottom portion of a bifurcated SEN was studied where deflection of flow decides the port outflow [13]. According to the authors, the port tube consists of at least two exit ports and provides more effective rotational flow inside the moulds from which molten metal flows from the port

tube. Results indicated that flow rotation increases the residence time inside the liquid mould pool for producing better floatation of the inclusions and also reduces the dendrites growth which formed along the steel solidifying [14].

The research of Pieprzyca et al. focusses on the escalation of submerged entry nozzle depth in the continuous casting mould. The way at which molten steel flux and also the speed of flowing molten steel into the mould in the continuous casting process plays an important role [15]. Sen et al. observed that continuous casting production of steel in defect-free form was the demand of each and every steelmaker. According to the authors, due to non-metallic inclusions, defects are formed in the steel. Steel turbulence must be such that more and more impurities will be floating near the meniscus of the mould and they are apprehended by the casting powder, and turbulence must not be high enough for capturing the particles of casting powder inside the liquid steel [16]. Ramos et al. investigated two different bifurcated submerged entry nozzles having a rectangular port and a square port and having an immersion depth of 115 mm and 185 mm, taken for study and having a 1:1 scale ratio. Rectangular ports possess optimum velocity spikes per minute, having greater magnitudes rather than using square SEN [17]. Ghaleni et al. studied the behaviour of fluid flow patterns and turbulence inside a slide gate; a throttled submerged entry nozzle was studied using the Detached-Eddy Simulation (DES) model. Results showed DES models as having notable rewards over the standard k-epsilon turbulence model model in the case of transient simulations [18]. The results of Zhang et al. indicated that when the immersion depth of the submerged entry nozzles increases, molten steel fluctuations near the surface decrease. When the depth of immersion of the submerged entry nozzle was deeper, the velocity of the molten steel near the surface was found to be slower and the temperature was also low which results in the meniscus becoming too cold and also stagnant [19]. According to Kohei and Yuji, to evaluate the effects of the electromagnetic brake under high molten steel flow rate conditions, the momentum of molten steel in a mould with two static magnetic fields in the flow control mould was investigated [20]. Timmel et al. deal with numerical simulations and model experiments related to the behaviour of the fluid flow pattern during the continuous casting process in the steel making process. According to the authors, ultrasonic, inductive techniques, and X-ray radioscopy were employed for the quantification of flow or the visualizations of two-phase flow regimes occurring in the submerged entry nozzle and the mould [21].

In this current study, a laboratory design of a continuous casing machine has been modeled and constructed toward implementation of an experiment under different variables like water flow rate, different mould section size, and different submerged entry nozzle port angle. Analysis provides persistent investigation results because laboratory design is not affected by the type and composition of the produce. In this experiment, the chief objectives are (i) performing an experiment to measure the meniscus fluctuation under different mould section size, and different submerged entry nozzle port angle under different operating conditions, and (ii) to conduct a comparative analysis of the various parameters for the proposed system.

2. Similarity Criteria

Considering the situation that occurs at the process plant in a laboratory, a working model of the real system has to be made. To simulate the real process, there are some criteria that have to be fulfilled. For a model to describe a real situation well, we must ensure the quality of the dimensionless numbers. The ratio of forces occurring in a system can be expressed by the dimensionless numbers, which in turn serve as similarity parameters for a scale down of SEN and mould equipment. Generally, we are balancing force ratios between the model and the prototype to maintain similitude. Dynamic similarity ensures that interactions between the forces which occur in the mould will also occur in the same fashion in the actual system.

The primary motivation for carrying out reduced scale model studies, ideally speaking, is to predict certain phenomena in the full scale steel processing system using appropriate

scale up correlations. This, however, is often not possible to achieve since the physical models applied are often inexact, and hence, the corresponding scale up correlations are somewhat uncertain.

Water modelling of a system can easily be carried out by constructing a model on smaller scale. This is done by making use of scale factor, λ . This makes the system a lot cheaper and convenient to work with. A full scale water model requires no velocity scaling due to the dynamic similarity between liquid steel and water, as they share approximately the same kinematic viscosity. It is impossible to satisfy all the requirements of similarity of fluid flow during continuous casting in a single model due to limitations of water modelling and the diversity of flow phenomena. However, the Froude number alone can be satisfied at any scale in a ladle/tundish/mould water model as long as all the geometrical and fluid hydraulic heads in the system are varied with a single scaling parameter.

The present study is carried out on a slab caster mould, and the entire set-up consisting of SEN and mould was built with a scale factor of 0.33 scale. The velocity was scaled down using Froude similarity. Every length dimension in the water-model was scaled down as

$$L_{\text{model}} = \lambda L_{\text{prototype}} \quad (1)$$

Since the system is assumed to be Froude number dominated, velocity and flow rate in the model and full scale system are expressed as

$$Fr_{\text{model}} = Fr_{\text{proto}} \quad (2)$$

$$Q_{\text{model}} = \lambda^{\frac{5}{2}} Q_{\text{proto}} \quad (3)$$

where V_{model} and V_{proto} are the velocities at corresponding points in the model and prototype, respectively; Q_{model} and Q_{proto} are flow rates at corresponding points in the model and prototype respectively; D_{model} and D_{proto} are the diameters of the SEN of the model and prototype, respectively; Fr_{model} and $Fr_{\text{prototype}}$ represent the Froude Number in the model and prototype, respectively.

3. Material and Methods

3.1. Experimental Setup

The study was carried out using a 0.33 scaled down model of Perspex where all the dimensions of the SEN and mould were scaled down by 0.33, respectively. The model dimensions of SEN and mould are shown in Table 2.

Table 2. Dimension of industrial and scaled-down models of slab caster.

| Parameters | Industrial | Scale Down Model ($\lambda=0.33$) |
|--|------------|-------------------------------------|
| Mould width, mm | 1500 | 500 |
| Mould thickness, mm | 210 | 70 |
| Mould length, mm | 1200 | 1200 |
| Submerged Entry Nozzle (SEN) bore diameter, mm | 75 | 25 |
| Port width, mm | 55 | 20 |
| Port height, mm | 100 | 33 |
| Port angle | 0° | 0, −15°, 15° |

The pictorial view and experimental setup constructed at Birla Institute of Technology, Mesra Ranchi, used to perform the experiments are shown in Figure 1a,b. The mould is made up of Perspex sheets. The size of the mould has a dimension of $(1200 \times 500 \times 70) \text{ mm}^3$ fixed in a metallic frame. The mould length was taken as 1200 mm, for a better simulation of flow in the lower portion of the mould. A cylindrical tank was placed over the metallic frame to act as a tundish. A valve was installed at the outlet of the tundish to regulate the liquid flow. A Submerged Entry Nozzle (SEN) has been installed at the tundish axis to

discharge water into the Perspex glass mould. At the exit, the SEN was bifurcated as two outlet ports. To provide the well depth in the SEN, an adjustable pipe cap was installed in the lower part of the SEN. The liquid steel discharged from the port into the mould towards the narrow side wall of the mould. The experiment was carried out by filling up the mould with water by opening the valve and starting the pump. Once the water was filled up in the mould up to the required level, the valve was closed. Fine control of water levels in the mould was achieved either by taking out some amount of water from the bottom of the mould by opening the tap or by adding some amount of water from the top of the mould. The whole process took roughly 20 minutes to achieve a steady state. Methylene blue dye was added into the mould to colour the tap water blue to get a better picture of the surface fluctuations. A digital camera was used to get a better picture of the surface fluctuation. At a steady state, the maximum wave fluctuations were recorded at seven different locations on one half of the mould. It was assumed that flow was asymmetrical in the mould around the Submerged Entry Nozzle.

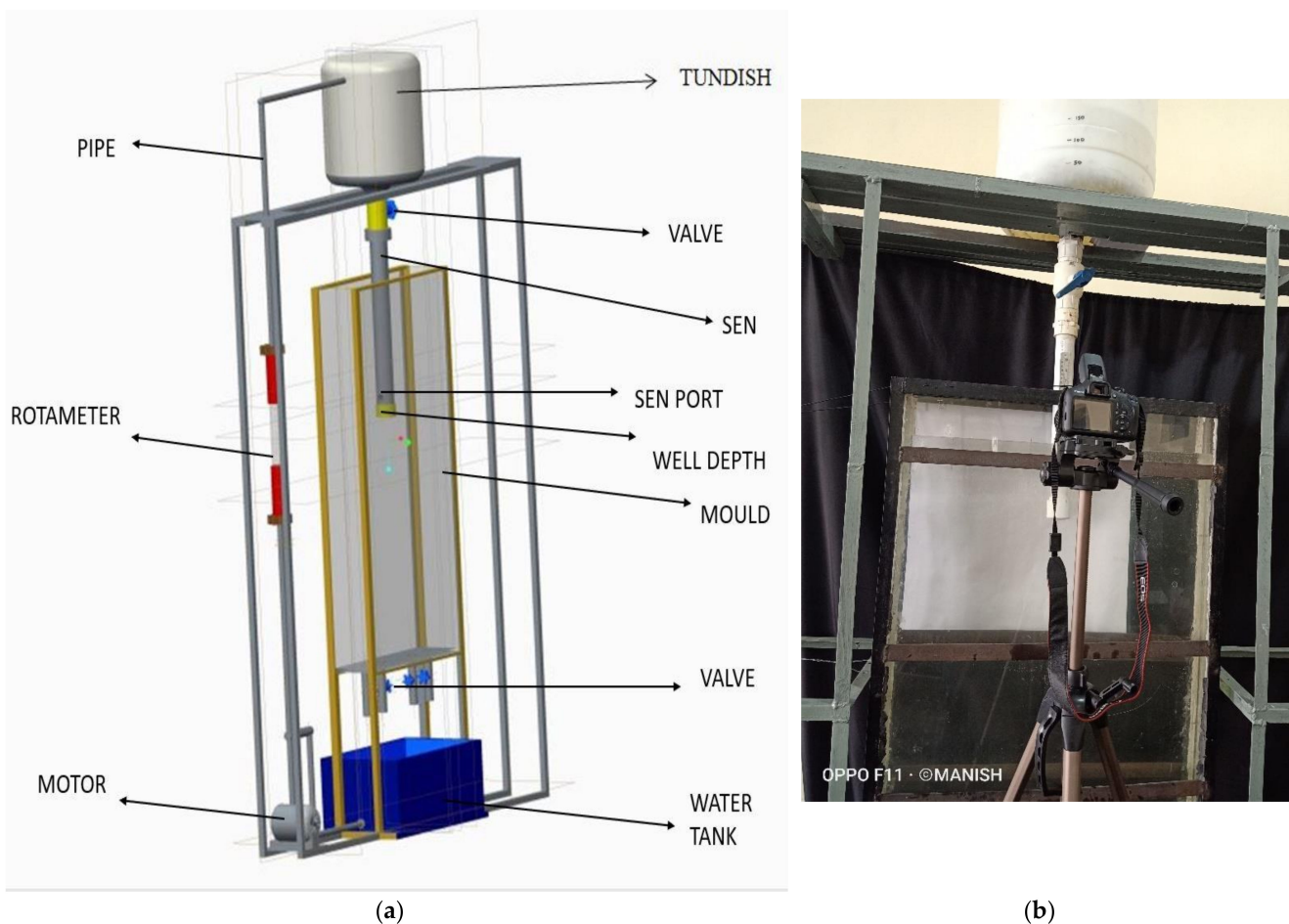


Figure 1. (a) Pictorial view of the water model experimental setup. (b) Experimental setup at the Department of Mechanical Engineering, Birla Institute of Technology, Mesra (Ranchi), India.

3.2. Instrumentation and Specification

The components and its specification used in the experimental setup are shown in Table 3.

Table 3. The components and specification of the experimental setup are as follows:

| Components | Specification and Function |
|-----------------------------|--|
| 1. Cylindrical tundish tank | Acts as tundish to store water at desired level and is cylindrical in shape. The thickness of the cylindrical vessel taken was 5 mm |
| 2. Mould | Most important part of the experiment setup. Meniscus fluctuation and flow visualization takes place inside the mould. Thickness: 12 mm; and mould dimensions: (1200 × 500 × 70) mm ³ |
| 3. Water outlet tank | The Perspex mould was connected to the water outlet tank with the help of a valve arrangement |
| 4. SEN | It has a straight through bore having a bifurcated outlet port |
| 5. Rota meter | Range 0–100 L/min |
| 6. Water circulating pump | Horse power motor |
| 7. Digital camera | Canon camera 1500D |
| 8. Pipes | 1 inch pipe having a length of 10 feet |

4. Result and Discussion

Water model experiments were performed to study the effects of mould section sizes, three different SEN_s, liquid flow rates through the SEN, on surface fluctuations in the mould. The video recording of the meniscus for each experiment was done and analysis of the meniscus was carried out at seven different locations in one half of the mould. The maximum meniscus fluctuation at each location was calculated by taking an average of 20 values at that time. The difference between the crest and trough is defined as the wave amplitude. The recorded video of surface fluctuations was downloaded into the computer for computation of average and maximum wave amplitude. A total of 100 frames in a sequence were downloaded from video for further analysis. Each frame was analysed individually. The data have been analysed for the prediction of average wave amplitude and maximum wave amplitude. The displacement of each point was first calculated with respect to a reference line. The reference line was chosen in such a way that all points fall above that line. This was done for the convenience of computation because our interest was in the wave amplitude. As mentioned earlier, the average meniscus displacement at each point was computed by taking an average of 20 points. This point kept on fluctuating during the measurement. The uncertainty in the measurement of this point was computed by taking the average and standard deviation of 20 values.

The comparative analysis of standard deviation from the present setup was done with different investigators as shown in Figures 2 and 3.

Figures 4 and 5 show the fluctuations of the meniscus wave at the crest and trough with respect to time for 0° and 15° downward port nozzles at the same conditions as abovementioned. For the parallel port, the difference between the crest and trough, i.e., amplitude, was found to be less in comparison with the 15° downward ports. However, the wave fluctuations at a particular location, either crest or trough, was found to be more in case of the parallel port nozzle compared to the 15° downward ports.

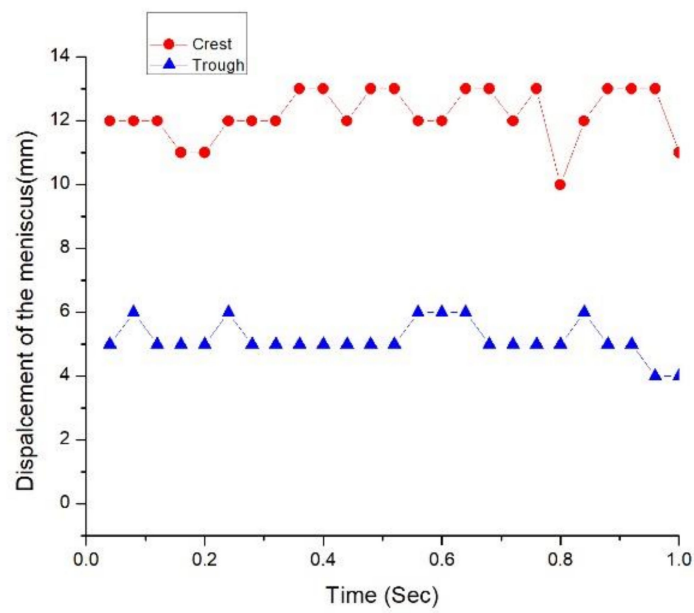


Figure 2. Comparison of the standard deviation of the meniscus along the mould width for 0° rectangular port nozzles with a different investigator.

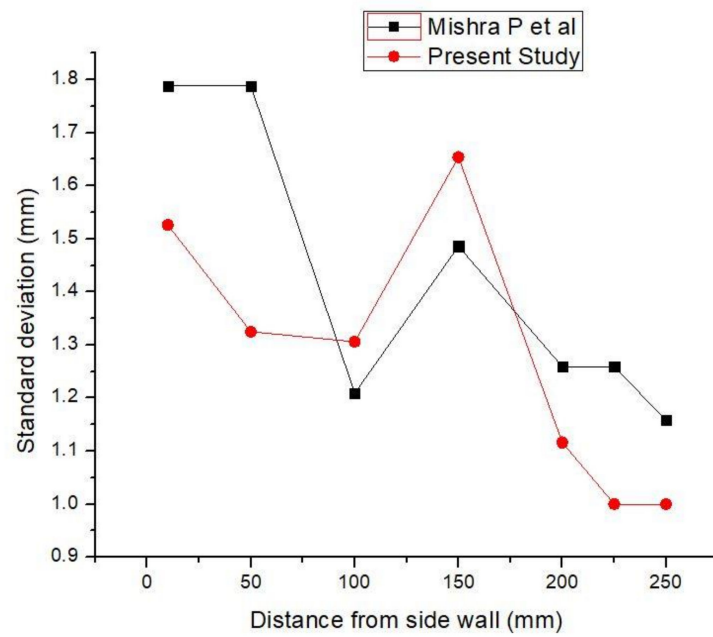


Figure 3. Comparison of the standard deviation of the meniscus along the mould width for 15° downward rectangular port nozzles with a different investigator.

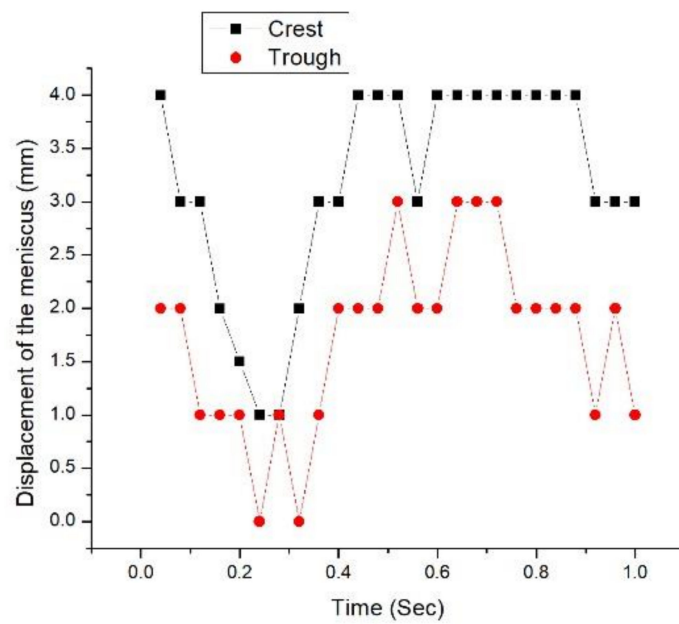


Figure 4. Displacement of meniscus at crest and trough in one second for 0° rectangular port nozzle.

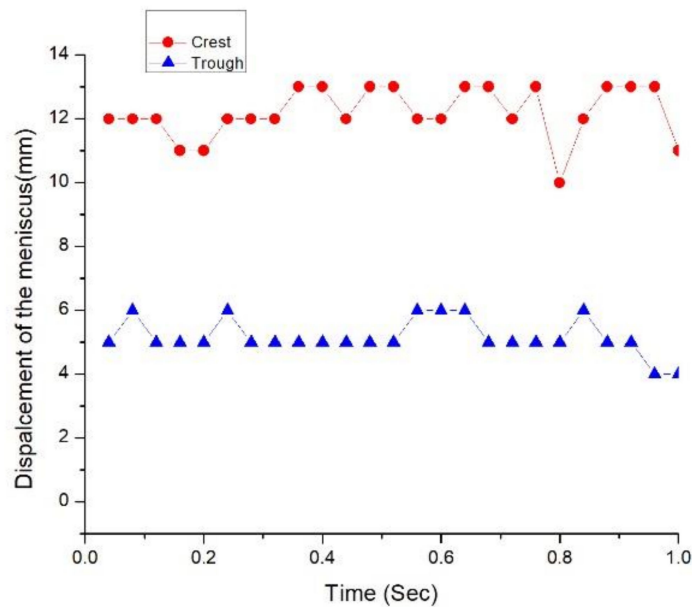


Figure 5. Displacement of the meniscus at crest and trough in one second for 15° downward rectangular port nozzle.

4.1. Maximum Meniscus Profile for Different Section Size

The maximum meniscus profile generated for each experiment was used to compute the maximum surface wave amplitude. From the recording, different photographs were taken out, and by using an image processor (MATLAB, R2012a, Mathworks, Natick, MA, USA), various images of meniscus fluctuation were obtained, as shown in Figure 6. It was observed that at a high flow rate of 60 L/min when compared to 40 L/min, there was a clear change in the maximum wave amplitude.

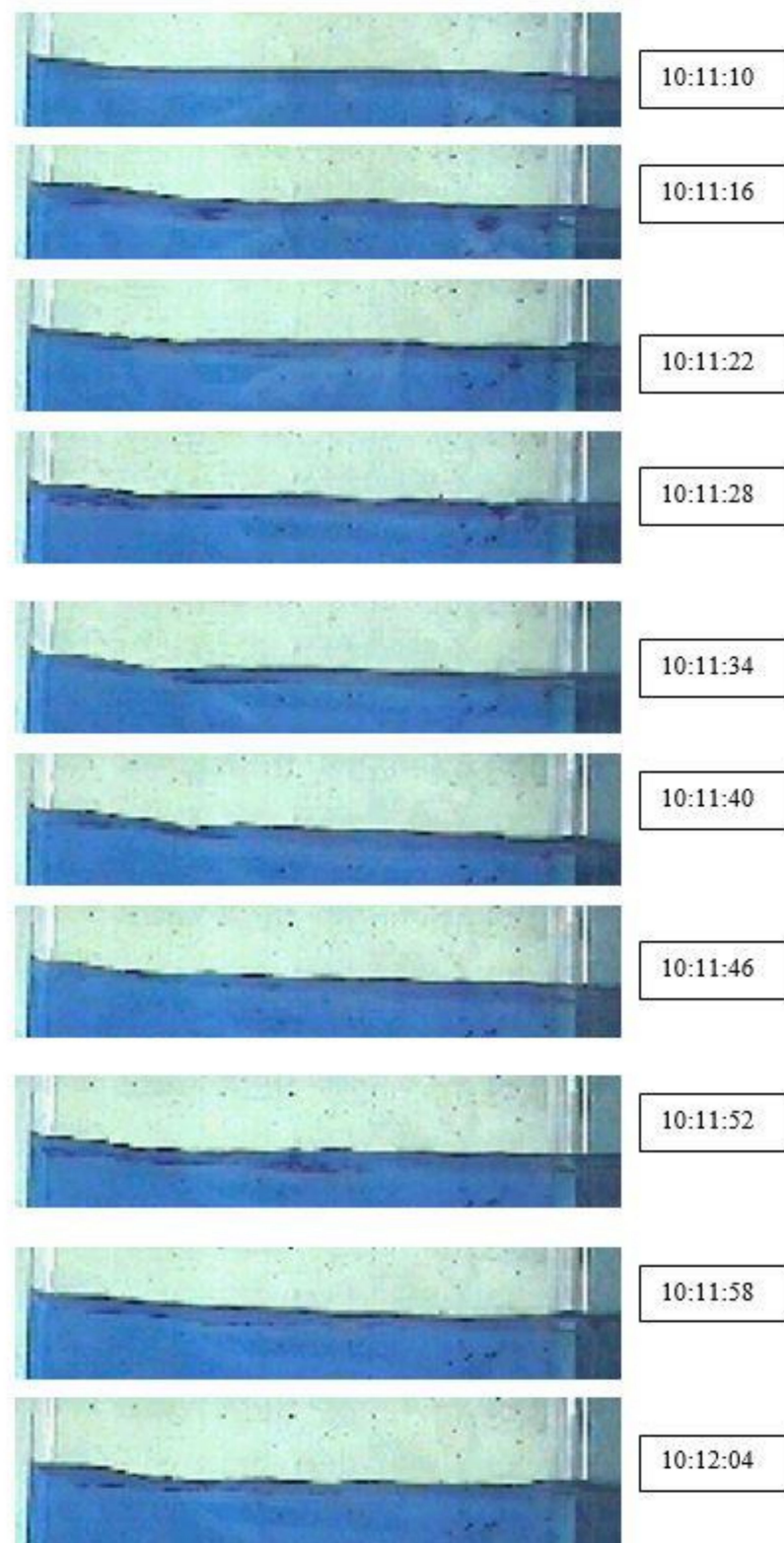


Figure 6. Various images of meniscus fluctuation were obtained from MATLAB coding.

4.2. Effect of Different Section Sizes on Surface Fluctuation

Experiments were performed for four different section sizes (500 mm, 433 mm, 350 mm, and 316 mm) with three different SEN_S (0° , 15° downward, and 15° upward ports) under different liquid flow rates from the SEN. Different conditions of liquid flow rates were 40 L/min and 60 L/min from SEN. Figure 7 shows the maximum surface wave amplitude

for a 0° port nozzle. The maximum surface wave amplitude increased with the increase of section size from 316 mm to 350 mm under all the conditions. However, an increase in the maximum wave amplitude with the liquid flow rate of 60 L/min from SEN was much higher when compared. From Figures 7–9 it can be seen that the nature of the curves remained very similar. The minimum wave fluctuation was found to be 2.8 mm at a flow rate of 40 L/min for the 0° port under the mould section of 316 mm. The maximum wave fluctuation found was to be 15.8 mm at a flow rate of 60 L/min for the 15° downward port under the mould section of 350 mm.

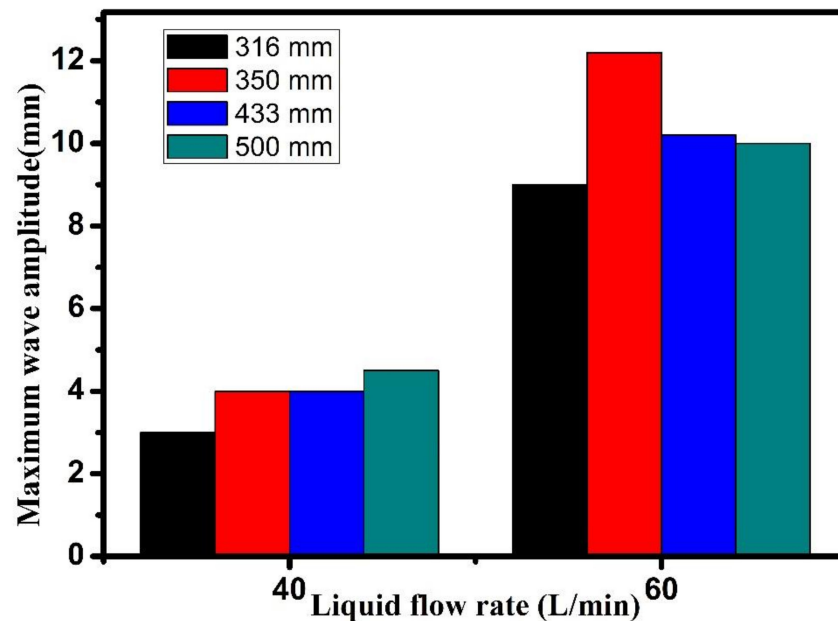


Figure 7. Effect of section size (mould width) on maximum surface wave amplitude for 0° port under different operating conditions.

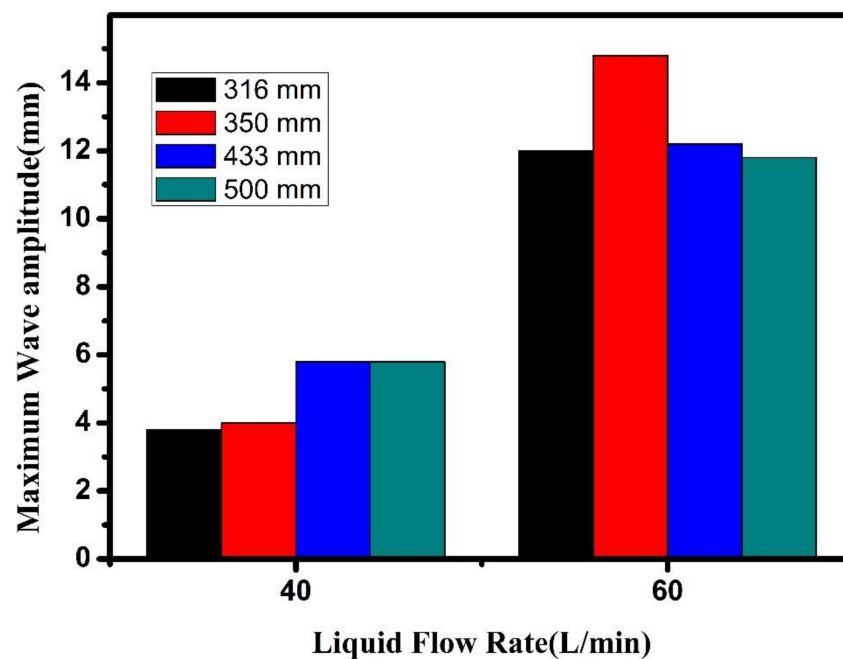


Figure 8. Effect of section sizes (mould width) on maximum surface wave amplitude for 15° downward port under different operating conditions.

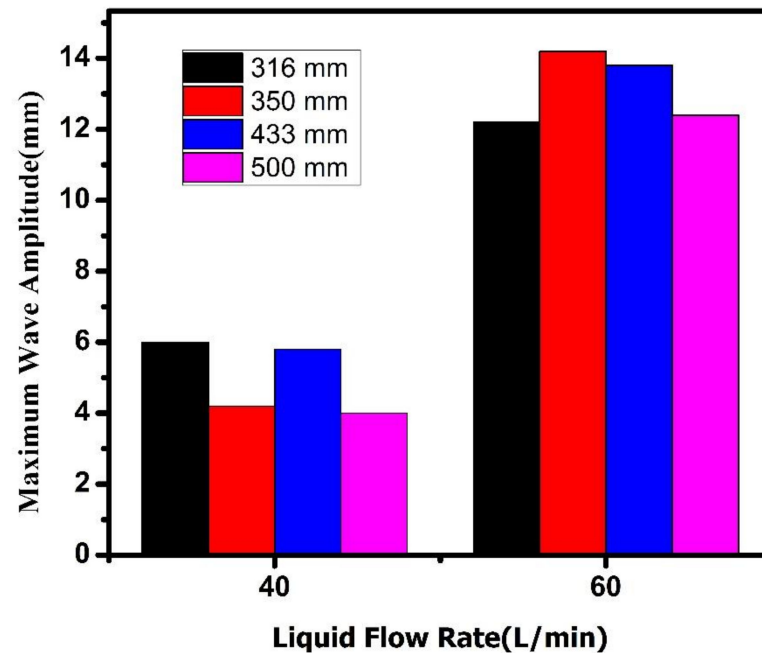


Figure 9. Effect of section sizes (mould width) on maximum surface wave amplitude for 15° upward port under different operating conditions.

4.3. Effect of Different Submerged Entry Nozzles on Surface Fluctuations

Generally, it was expected that the nozzle with a downward angle would give lower meniscus fluctuation compared to the 0° port nozzle. It was found, though, that the nozzle with a downward angle gave a higher maximum fluctuation.

Figures 10 and 11 compare the performance of three different SENs, 0°, 15° downward, and 15° upward, at four different section sizes and operating conditions with respect to the maximum surface wave amplitude. It can be observed from the Figures 10 and 11 that the maximum surface wave amplitude increased with the change of SEN from 0° to 15° downward with most of the section sizes. However, the maximum surface wave amplitude decreased with some of section size (350 mm) as the nozzle was changed from 0° to 15° downward nozzle.

At the liquid flow rate of 40 L/min from SEN, the maximum surface wave amplitude increased with the change of nozzle from 0° to 15° downward nozzle and section size beyond 350 mm. The maximum surface wave amplitude remained the same with a 15° upward nozzle as compared with a 15° downward nozzle with many of the operating conditions and section sizes. It was observed that the maximum surface wave amplitude at the lower section size (350 mm) either increased or remained constant with the change of nozzle to 15° upward compared to a 15° downward nozzle and at all the operating conditions considered. At a higher section size (350 mm and above), the maximum surface wave amplitude either remained constant or decreased with a 15° upward nozzle compared to a 15° downward nozzle at all operating conditions. A higher flow rate leads to a higher surface wave in the mould, which results in higher upward velocities. An increase in momentum of the liquid jet leads to an increase in surface wave amplitude [22].

It can be concluded from Figure 10 that a 0° nozzle gives lower maximum surface wave amplitude compared to a 15° downward nozzle for a mould section size more than 350 mm at lower liquid flow rates. The minimum wave fluctuation found was 2 mm at a 0° port nozzle at 40 L/min flow rates under a mould section size of 316 mm. The maximum wave fluctuation was 14.6 mm at a 15° downward port nozzle at 60 L/min flow rates under a mould section size of 350 mm.

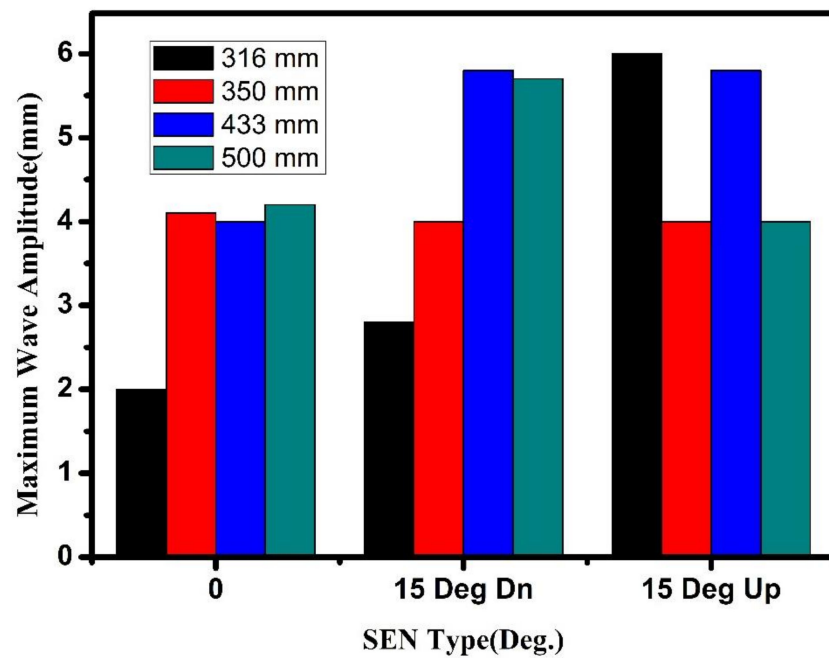


Figure 10. Variation of maximum surface wave amplitude with different nozzle types at 40 L/min liquid flow rate from Submerged Entry Nozzle (SEN) at different mould width.

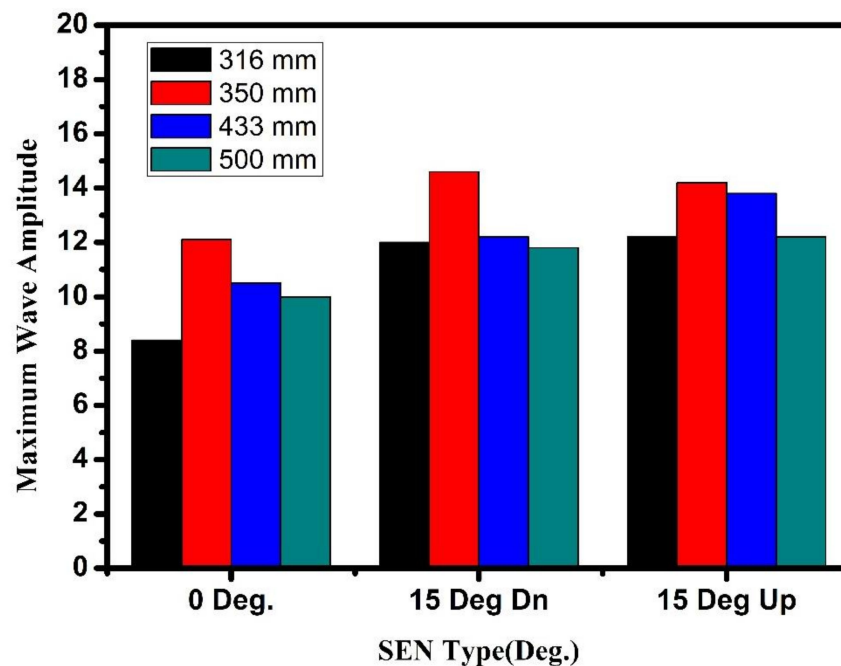


Figure 11. Variation of maximum surface wave amplitude with different nozzle types at 60 L/min liquid flow rate from SEN at different mould width.

5. Conclusions

In the present analysis, water model experiments were carried out in a model with a scale-down ratio of 0.33. The present investigation shows how different types of mould section size and different SEN port angles affect meniscus fluctuation and further provides necessary background information for the steel maker. Based on the experiment performed and the above analysis, the following conclusion has been made.

The meniscus profile was wavy with a crest and a trough on either side of the nozzle. It keeps on fluctuating at any casting speed.

The maximum and average wave amplitude was increasing with the decrease in submergence depth.

A submerged entry nozzle with a 0° port was found to be superior compared to 15° downward and 15° upward nozzles.

As the water flow rate increased, the maximum wave amplitude was found to be increasing, which results in more turbulence. It was clear from the observation that a 15° downward port nozzle has higher maximum wave amplitude compared to a 0° port nozzle. Due to a strong upper recirculation zone, the water reached to the meniscus with higher momentum and gave more fluctuations at the meniscus.

The maximum wave amplitude was found to be much higher at 60 L/min compared to a 40 L/min water flow rate. For all three nozzles (0°, 15° downward, and 15° upward), 15° downward and 15° upward nozzles were found to give a higher maximum wave amplitude compared to the 0° port at all the flow rates studied.

When the flow rate of liquid was 40 L/min, the maximum surface wave amplitude increased with the change of nozzle from 0° to 15° downward nozzle and section size beyond 350 mm.

It was observed that the maximum surface wave amplitude at the lower section size (316 mm) either increased or remained constant with the change of nozzle to 15° upward compared to a 15° downward nozzle and at all the operating conditions considered. At a higher section size (350 mm and above), the maximum surface wave amplitude either remained constant or decreased with a 15° upward nozzle compared to a 15° downward nozzle at all operating conditions.

Author Contributions: Conceptualization, M.K. and P.M.; methodology, M.K.; software, M.K.; validation, M.K., P.M., and A.K.R.; formal analysis, M.K.; investigation, M.K., P.M.; resources, M.K.; data curation, M.K., P.M.; writing—original draft preparation, M.K.; writing—review and editing, M.K., P.M., and A.K.R.; visualization, M.K.; supervision, P.M. and A.K.R. All authors have read and agreed to the published version of the manuscript.

Funding: This research received external funding by University Grant Commission under the scheme of NFOBC (Student Id= MANISH KUMAR (201819-NFO-2018-19-OBC-BIH-74425)).

Data Availability Statement: Data is contained within the article.

Acknowledgments: The experimental work was supported by the Department of Mechanical Engineering, Birla Institute of Technology, Mesra (Ranchi), India.

Conflicts of Interest: The authors declare no conflict of interest.

References

1. Chen, Y.; Zhang, L.; Yang, S.; Li, J. Water modeling of self-braking submerged entry nozzle used for steel continuous casting mold. *JOM* **2012**, *64*, 1080–1086. [[CrossRef](#)]
2. Fang, Q.; Ni, H.; Zhang, H.; Wang, B.; Lv, Z. The effects of a submerged entry nozzle on flow and initial solidification in a continuous casting bloom mold with electromagnetic stirring. *Metals* **2017**, *7*, 146. [[CrossRef](#)]
3. Cui, H.; Zhang, J.W.; Liu, J.H.; Su, W.; Yan, J.B.; Wang, F.L. Effect of submerged entry nozzle structure on fluid flow in a beam blank continuous casting mould. *Ironmak. Steelmak.* **2010**, 1–10. [[CrossRef](#)]
4. Real-Ramirez, C.A.; Gonzalez-Trejo, J.I. Analysis of three-dimensional vortexes below the free surface in a continuous casting mold. *Int. J. Miner. Metall. Mater.* **2011**, *18*, 397. [[CrossRef](#)]
5. Michalek, K.; Gryc, K.; Tkadlečková, M.; Morávka, J.; Huczala, T.; Bocek, D.; Horáková, D. Type of submerged entry nozzle vs. concentration profiles in the intermixed zone of round blooms with a diameter of 525 mm. *Mater. Technol.* **2012**, *46*, 581–587.
6. Liu, R.; Thomas, B.G.; Sengupta, J. Simulation of Transient Fluid Flow in Mold Region During Steel Continuous Casting. In Proceedings of the IOP Conference Series: Materials Science and Engineering, Schladming, Austria, 17–22 June 2012; Volume 33, p. 012015.
7. Real-Ramirez, C.A.; Miranda-Tello, R.; Hoyos-Reyes, L.; Reyes, M.; Gonzalez-Trejo, J.I. *Numerical Evaluation of a Submerged Entry Nozzle for Continuous Casting of Steel*; NISCAIR-CSIR: New Delhi, India, 2012.
8. Cho, S.M.; Kim, S.H.; Thomas, B.G. Transient fluid flow during steady continuous casting of steel slabs: Part I. Measurements and modeling of two-phase flow. *ISIJ Int.* **2014**, *54*, 845–854. [[CrossRef](#)]
9. Li, D.; Su, Z.; Chen, J.; Wang, Q.; Yang, Y.; Nakajima, K.; He, J. Effects of electromagnetic swirling flow in submerged entry nozzle on square billet continuous casting of steel process. *ISIJ Int.* **2013**, *53*, 1187–1194. [[CrossRef](#)]

10. Begum, L.; Hasan, M. 3-D CFD simulation of a vertical direct chill slab caster with a submerged nozzle and a porous filter delivery system. *Int. J. Heat Mass Transf.* **2014**, *73*, 42–58. [[CrossRef](#)]
11. Ren, Y.; Wang, Y.; Li, S.; Zhang, L.; Zuo, X.; Lekakh, S.N.; Peaslee, K. Detection of non-metallic inclusions in steel continuous casting billets. *Metall. Mater. Trans. B* **2014**, *45*, 1291–1303. [[CrossRef](#)]
12. Yingnakorna, T.; Khumkoaa, S. Corrosion Behaviour of Submerged Entry Nozzle(SEN) During Continuous Casting of Steel. *Global Illuminators* **2014**, *1*, 62–69.
13. Pirker, S.; Kahrimanovic, D.; Schneiderbauer, S. Secondary Vortex Formation in Bifurcated Submerged Entry Nozzles: Numerical Simulation of Gas Bubble Entrapment. *Metall. Mater. Trans. B* **2015**, *46*, 953–960. [[CrossRef](#)]
14. Richaud, J.L. U.S. Patent No. 9,120,148, 2015.
15. Pieprzyca, J.; Merder, T.; Saternus, M. Optimization of Submerged Entry Nozzle Depth in CC Mould/Optymalizacja Zanurzenia Wylewu W Krystalizatorze Cos. *Arch. Metall. Mater.* **2015**, *60*, 2927–2932. [[CrossRef](#)]
16. Sen, A.; Prasad, B.; Sahu, J.K.; Tiwari, J.N. Designing of Sub-entry Nozzle for Casting Defect-free Steel. In Proceedings of the IOP Conference Series: Materials Science and Engineering, Rourkela, India, 5–6 December 2015; Volume 75, p. 012006.
17. Calderón-Ramos, I.; Morales, R.D. The role of submerged entry nozzle port shape on fluid flow turbulence in a slab mold. *Metall. Mater. Trans. B* **2015**, *46*, 1314–1325. [[CrossRef](#)]
18. Mohammadi-Ghaleni, M. Computational Fluid Dynamics (CFD) Simulations of Molten Steel Flow Patterns and Particle-Wall Adhesion in Continuous Casting of Steels. Master's Thesis. 2016.
19. Zhang, J.; Zhang, C.Q.; Wang, L.; Han, M.R.; Hwang, W.S. Automatic Control of Slag Line for Submerged Entry Nozzle (SEN). *Metallurgist* **2017**, *60*, 916–922. [[CrossRef](#)]
20. Furumai, K.; Miki, Y. Molten steel flow control technology for decreasing slab defects. *JFE Gihō*. **2016**, *38*, 36–41.
21. Timmel, K.; Kratzsch, C.; Asad, A.; Schurmann, D.; Schwarze, R.; Eckert, S. Experimental and Numerical Modeling of Fluid Flow Processes in Continuous Casting: Results from the LIMMCAST-Project. In Proceedings of the Final LIMTECH Colloquium and International Symposium on Liquid Metal Technologies, Dresden, Germany, 19–20 September 2017; Volume 228, p. 012019.
22. Kumar, M.; Mishra, P.; Kumar Roy, A. Influence of Submerged Entry Nozzle Port Blockage on the Meniscus Fluctuation Considering Various Operational Parameters. *Metals* **2020**, *10*, 269. [[CrossRef](#)]